Pharm Res (2013) 30:16–24
DOI 10.1007/s11095-012-0819-0

RESEARCH PAPER

Following the Concentration of Polymeric Nanoparticles During Nebulization

Moritz Beck-Broichsitter • Marie-Christine Knuedeler • Thomas Schmehl • Werner Seeger

Received: 16 March 2012 / Accepted: 20 June 2012 / Published online: 18 July 2012
© Springer Science+Business Media, LLC 2012

ABSTRACT

Purpose Nebulization represents one strategy to achieve pulmonary deposition of biodegradable nanoparticles. Besides stability as a key requirement to maintain functionality, the output of nanoparticles from the nebulizer needs to be considered to facilitate an efficient pulmonary therapy.

Methods Formulations nebulized by air-jet and vibrating-membrane technology were analyzed for their aerodynamic characteristics by laser diffraction. The nebulization stability of poly(D,L-lactide-*co*-glycolide) nanoparticles was assessed by dynamic light scattering. Moreover, several methods were employed to account for the shift in solute and NP reservoir concentration during nebulization.

Results Regardless of the formulation or nebulizer used generated aerosols all showed aerodynamic characteristics suitable for deep lung deposition. However, nanoparticles were prone to aggregation and concentrated during air-jet nebulization. The particle concentration effect was significantly pronounced in comparison to molecular solutes under the same nebulization conditions, due to nanoparticle aggregation and subsequent particle remainder in the reservoir. In contrast, vibrating-membrane technology did not affect nanoparticle integrity and reservoir concentration during nebulization, as the unaffected submicron particles passed through the tapered holes of the actuated plate.

Conclusions Aggregation and concentration effects during air-jet nebulization emphasize that nanosuspensions should preferably be delivered with a suitable vibrating-membrane device in order to ensure an effective pulmonary application.

M. Beck-Broichsitter (✉) · M.-C. Knuedeler · T. Schmehl · W. Seeger
Medical Clinic II, Department of Internal Medicine
Justus-Liebig-Universität Giessen
Klinikstrasse 33
35392 Giessen, Germany
e-mail: moritz.beck-broichsitter@innere.med.uni-giessen.de

KEY WORDS aggregation · biodegradable nanoparticles · concentration changes · pulmonary drug delivery · vibrating-membrane nebulization

ABBREVIATIONS

CF	5(6)-carboxyfluorescein
DLS	dynamic light scattering
DMSO	dimethyl sulfoxide
FPF	fine particle fraction
GSD	geometric standard deviation
LDA	laser Doppler anemometry
MWCO	molecular weight cut-off
NP	nanoparticles
PDI	polydispersity index
PLGA	poly(D,L-lactide-*co*-glycolide)
S.D.	standard deviation
TEM	transmission electron microscopy
THF	tetrahydrofuran
UV/Vis	ultra violet/visible
VMD	volume median diameter

INTRODUCTION

Over the past decades pulmonary drug delivery has gained considerable attraction as an avenue for the treatment of local and systemic diseases (1,2). However, the effective clearance mechanisms present in the respiratory tract cause a rapid decay of pulmonary drug concentration (3,4). The administration of drug-loaded biodegradable nanoparticles (NP) to the lung represents one strategy to circumvent multiple daily inhalations (up to 9 times per day) (5), a significant disadvantage of "conventional" inhalation therapy, as these delivery vehicles are able to bypass macrophage clearance (4) and release the encapsulated drug in controlled fashion (6–10).

Therapeutic aerosols are commonly generated by means of pressurized metered dose and dry powder inhalers and medical nebulizers (11). Pneumatic- and ultrasound-driven nebulizers frequently used for aerosolization of aqueous formulations in the past demonstrate several operational disadvantages, among these high residual volumes, concentration of medicaments inside the nebulizer reservoir and consequently an inefficient drug therapy (12,13). Recent technological advances caused the development of nebulizers employing vibrating membranes for aerosol generation with the aim to ameliorate treatment modalities based on pulmonary drug application (13–15). Different methods have been evaluated for the inhalative delivery of NP (10,16), e.g. aerosolization of NP-containing microparticles (composite particles) (17–19) and nebulization of aqueous nanosuspensions (6,20–23). However, a number of formulations were prone to aggregation during nebulization (20,21,24), emphasizing that nanosuspensions should only be used in combination with a specific nebulizer. Although concentration of dispersed microparticles during nebulization was reported for both air-jet and ultrasonic nebulizers (25), scant information is available on the change of NP concentration during aerosolization using vibrating-membrane technology.

Therefore, the present study addressed the change of NP concentration during nebulization with an air-jet (PARI LC SPRINT® STAR) and two actively vibrating-membrane (Aeroneb® Pro and eFlow®rapid) devices. Nebulization effects on aerodynamic characteristics of formulations were investigated by laser diffraction and the output rate was determined by gravimetric analysis. The change of solute concentration during aerosolization was followed using an internal standard. NP were prepared by a nanoprecipitation technique and characterized by dynamic light scattering and transmission electron microscopy before and after nebulization. Finally, the NP concentration inside the nebulizer reservoir was monitored by different methods, i.e. spectrophotometry, gravimetric analysis and fluorescence spectroscopy.

MATERIALS AND METHODS

Materials

Poly(D,L-lactide-*co*-glycolide) (PLGA), Resomer® RG 502 H was acquired from Boehringer Ingelheim (Ingelheim, Germany). Poloxamer 188 (Pluronic® F68), 5(6)-carboxyfluorescein (CF) (95%) and coumarin 6 (98%) were obtained from Sigma-Aldrich (Steinheim, Germany). All other chemicals and solvents used in the current study were of the highest analytical grade commercially available.

Methods

Preparation of NP

PLGA NP with nominal sizes of 100 and 200 nm were synthesized by a nanoprecipitation technique (26). For the preparation of PLGA100 NP, Resomer® RG 502 H was dissolved in dimethyl sulfoxide (DMSO) at a concentration of 30 mg/ml; for the preparation of PLGA200 NP, Resomer® RG 502 H was dissolved in tetrahydrofuran (THF) at a concentration of 20 mg/ml. The resulting polymer solutions (1.5 ml in both cases) were subsequently injected (injection needle: Fine-Ject® 0.6×30 mm) into a magnetically stirred (500 rpm) aqueous phase of 5 ml containing 0.1% Pluronic® F68 using a peristaltic pump (flow rate: 10.0 ml/min). After injection of the organic phase, the resulting colloidal dispersion was stirred for 10 min and then transferred to a dialysis bag (MWCO: 50,000 Da, Spectra/Por® 6, Breda, Netherlands) to remove additives (water miscible organic solvent and excess of Pluronic® F68). The nanosuspension was filtered prior to use (1.2 μm) to remove aggregates. The actual NP concentration in suspension was assessed gravimetrically by lyophilizing aliquots of the purified nanosuspension. The concentration of the nanosuspensions was adjusted prior to the nebulization experiments.

Characterization of NP

Size and ζ-Potential Measurement. The particle size and size distribution of NP were measured by dynamic light scattering (DLS), and their ζ-potential was determined by laser Doppler anemometry (LDA) in 1.54 mM NaCl (Zetasizer NanoZS/ZEN3600, Malvern Instruments, Herrenberg, Germany).

Transmission Electron Microscopy (TEM). After deposition of nanosuspension droplets on a carbon-coated copper grid (S160-3, Plano, Wetzlar, Germany) samples were dried in vacuum. The morphology of NP was subsequently investigated using a transmission electron microscope (JEM-3010 TEM, JEOL, Eching, Germany) at an accelerating voltage of 300 kV.

Nebulization Experiments. Nebulization experiments were carried out using an air-jet (PARI LC SPRINT® STAR, PARI, Starnberg, Germany) and two actively vibrating-membrane (Aeroneb® Pro, Aerogen, Dangan, Galway, Ireland; eFlow®rapid, PARI, Starnberg, Germany) nebulizers under the following ambient conditions: temperature: 24±1°C; relative humidity: 60±10%. NaCl 0.9% (m/v) solution (B. Braun, Melsungen, Germany) served as a control in all experiments.

Aerosol Output. The total aerosol output was determined gravimetrically by weighing the nebulizer unit before and after each nebulization experiment. The resulting difference in weight was used to calculate the aerosol output rate in g/min.

Aerosol Particle Size Determination by Laser Diffraction. The volume median diameter (VMD) of the produced aerosol droplets was determined by laser diffraction (HELOS, Sympatec, Clausthal-Zellerfeld, Germany) (27). The geometric standard deviation (*GSD*) was calculated from the laser diffraction values according to the following equation

$$GSD = \sqrt{\frac{d_{84\%}}{d_{16\%}}},$$

where d_n is the diameter at the percentile n of the cumulative distribution (28). The fine particle fraction (FPF) is given as the aerosol volume fraction with particle sizes below 5.25 μm.

Quantification of Solute Concentration During Nebulization. The solute concentration in the nebulizer reservoir was determined using the internal standard CF, which was added to the initial nebulization fluid at a concentration of 2 μg/ml (12).

At predetermined time points, the concentration of CF in the nebulizer reservoir was assessed using a fluorescence plate reader (FL600, Bio-Tek, Bad Friedrichshall, Germany) equipped with the following filters: λ_{ex}=485/20 nm, λ_{em}=530/25 nm. The CF content was calculated via a calibration curve. Results are expressed as relative changes of solute concentration to the time point 0 min.

Quantification of NP Concentration During Nebulization. Aliquots from the nebulizer reservoir sampled at predetermined time points were measured for NP concentration by different methods, namely spectrophotometry, gravimetric analysis and fluorescence spectroscopy. Results are expressed as relative changes of NP concentration to the time point 0 min.

Spectrophotometry. Light transmittance of the samples was assayed at a wavelength of 630 nm (Ultrospec® 3000, Pharmacia Biotech, Freiburg, Germany). The NP concentration in each sample was calculated using a calibration curve.

Gravimetric Analysis. Samples of 1 ml nanosuspension were frozen at −80°C, thawed, and immediately centrifuged (16,873·g, Centrifuge 5418, Eppendorf, Hamburg, Germany) for 1 h at 25°C. After centrifugation the supernatant was carefully removed and the remaining pellet was freeze-dried (ALPHA 1-4 LSC, Christ, Osterode, Germany) until weight constancy (BP 211 D, Sartorius, Göttingen, Germany).

Fluorescence Spectroscopy. NP were loaded with fluorescent dye coumarin 6 (0.1% (m/m)) for the determination of concentration via fluorescence spectroscopy (29). Briefly, dried samples were dissolved in acetonitrile (a common solvent for PLGA and coumarin 6) and the amount of coumarin 6 was determined with a fluorescence spectrophotometer (LS50B, Perkin-Elmer, Rodgau-Jügesheim, Germany) equipped with the following alignments: λ_{ex}=440 nm (slit: 2.5 nm), λ_{em}=501 (slit: 2.5 nm). The coumarin 6 content was calculated using a calibration curve.

Statistics. All measurements were carried out in triplicate and values are presented as mean ± S.D. unless otherwise noted. Statistical calculations were carried out using the software SigmaStat 3.5 (STATCON, Witzenhausen, Germany). To identify statistically significant differences, one-way ANOVA with Bonferroni's post *t*-test analysis was performed. Probability values of $p<0.05$ were considered significant and marked with an asterisk.

RESULTS

Nebulization experiments were performed with an air-jet (PARI LC SPRINT® STAR) and two actively vibrating-membrane (Aeroneb® Pro and eFlow®rapid) nebulizers. The aerosol characteristics and output rates for isotonic NaCl solution as nebulization fluid are presented in Table I. The VMD obtained were 3.0±0.1 μm (mean ± S.D., n=4), 5.5±0.1 μm (mean ± S.D., n=4), and 4.6± 0.4 μm (mean ± S.D., n=4) for the PARI LC SPRINT® STAR, Aeroneb® Pro and eFlow®rapid nebulizer, respectively.

The GSD was <1.9 for all nebulizers tested. The maximum FPF was achieved with the air-jet nebulizer (~85%), whereas a subordinate FPF was obtained for both vibrating-

Table I Aerodynamic and Output Characteristics of Isotonic NaCl Solution Aerosolized with Different Nebulizer Units. Values are Presented as Mean ± S.D. (n=4)

Nebulizer unit	VMD[a]/μm	GSD[b]	FPF[c]/%	Output rate/g/min
PARI LC SPRINT® STAR	3.0±0.1	1.78±0.02	85.3±1.9	0.08±0.01
Aeroneb® Pro	5.5±0.1	1.87±0.02	47.2±1.2	0.44±0.04
eFlow®rapid	4.6±0.4	1.65±0.05	62.5±8.5	0.71±0.04

[a] Volume median diameter; [b] geometric standard deviation; [c] fine particle fraction

membrane nebulizers (Aeroneb® Pro: ~47%; eFlow®rapid: ~63%). The lowest output rate was observed for the PARI LC SPRINT® STAR, at ~0.08 g/min. A higher output rate of ~0.44 g/min was found for the Aeroneb® Pro, followed by the eFlow®rapid (~0.71 g/min).

The change of solute concentration in the nebulizer reservoir during aerosolization was examined utilizing the internal standard CF (Fig. 1). For the PARI LC SPRINT® STAR the increase in solute concentration was a function of both the additional gas flow rate employed during nebulization and nebulization time (Fig. 1a). While for an additional gas flow rate of 20 l/min a solute concentration of 154.6±8.8% (mean ± S.D., n=4) was determined after 10 min of nebulization, the increase in solute concentration was significantly lower at 0 l/min (109.8±2.0%; mean ± S.D., n=4). Time courses of nebulization for the air-jet device clearly illustrate an amplified rise in solute concentration when additional gas flows through the nebulizer device (Fig. 1a, inset).

Contrary to air-jet nebulization, the solute concentration in the reservoirs of both vibrating-membrane nebulizers remained unchanged over the investigated course of aerosolization (Fig. 1b, Aeroneb® Pro: 100.6±3.7% after 10 min (mean ± S.D., n=4); eFlow®rapid: 99.8±4.5% after 6 min (mean ± S.D., n=4)).

The biodegradable NP prepared for the current study were composed of PLGA and had a nominal size of 100 and 200 nm. Their physicochemical properties were evaluated by means of DLS, LDA and TEM. The results are presented in Table II and Fig. 2. Freshly-prepared PLGA100 and PLGA200 NP had a mean size of 104.0±2.2 nm (mean ± S.D., n=11) and 200.5 ±4.2 nm (mean ± S.D., n=4), respectively, narrow size distribution displayed by a polydispersity index (PDI) below 0.12, and negative ζ-potential of ~−30 mV.

TEM was used to visualize the NP and confirmed the results from DLS measurements.

Nebulization experiments were performed with PLGA100 and PLGA200 nanosuspensions of different concentrations (1, 2 and 5 mg/ml). The measured aerodynamic

Table II Physicochemical Characteristics of poly(D,L-lactide-*co*-glycolide) (PLGA) Nanoparticles (NP). Values are Presented as Mean ± S.D. (n≥4)

NP formulation	Size/nm	PDI[a]	ζ-Potential/ mV	Encapsulation efficiency of coumarin 6/%
PLGA100	104.0±2.2	0.110±0.018	−32.0±3.4	97.1±3.8
PLGA200	200.5±4.2	0.112±0.011	−33.3±2.3	96.3±2.0

[a] Polydispersity index

and output properties are reported in Table III. All formulations were nebulizable by both air-jet and vibrating-membrane nebulizers. The VMD for the different formulations ranged from 3.0±0.2 to 3.4±0.4 µm (mean ± S.D., n=4) and from 5.5±0.1 to 5.9±0.1 µm (mean ± S.D., n=4) for the PARI LC SPRINT® STAR and Aeroneb® Pro nebulizer, respectively. Nebulization of PLGA100 nanosuspension (2 mg/ml) with the eFlow®rapid yielded an aerosol particle size of 4.6±0.2 µm (mean ± S.D., n=4).

Similar to the VMD measured for the different NP formulations, only marginal changes of GSD and FPF were obtained, as compared to nebulized isotonic NaCl solution (Table I). However, the output rate for both vibrating-membrane nebulizers was significantly decreased (p<0.05).

The stability of PLGA100 and PLGA200 nanosuspensions (2 mg/ml) during air-jet and vibrating-membrane nebulization is illustrated in Fig. 3. Air-jet nebulization led to an increase in mean particle size for both formulations. By contrast, neither the Aeroneb® Pro nor the eFlow®rapid did alter the NP properties over the investigated time of nebulization.

The NP concentration was quantified by spectrophotometry, gravimetric analysis and fluorescence spectroscopy using aliquots from the nebulizer reservoirs at predetermined time points (Fig. 4). For fluorescence measurements the employed NP were loaded with the fluorescent dye coumarin 6 (0.1% (m/m)). The encapsulation efficiency of coumarin 6 in the prepared PLGA100 and PLGA200 nm NP

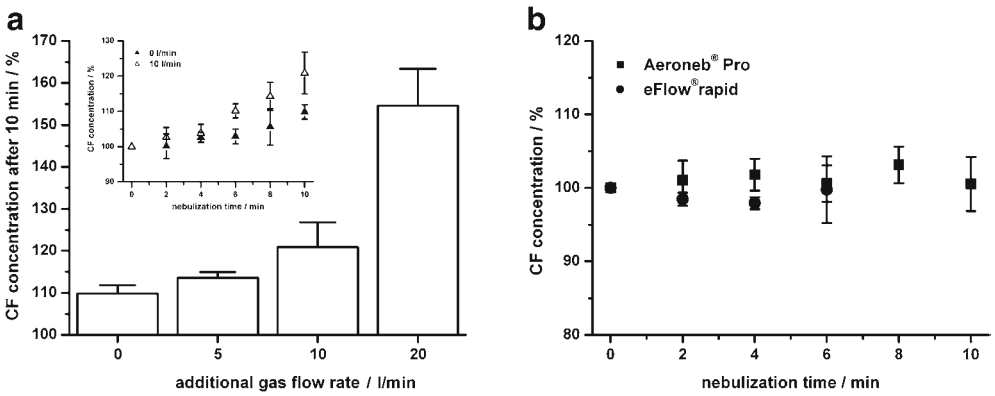

Fig. 1 Influence of nebulization time and additional gas flow rate on the concentration of the internal standard 5(6)-carboxyfluorescein (CF) in the reservoir fluid (NaCl 0.9% (m/v)) of the air-jet (PARI LC SPRINT® STAR) (**a**) and vibrating-membrane (**b**) nebulizers. The inset in (A) shows the time course of CF concentration for additional gas flow rates of 0 and 10 l/min, respectively. Values are presented as mean ± S.D. (n=4).

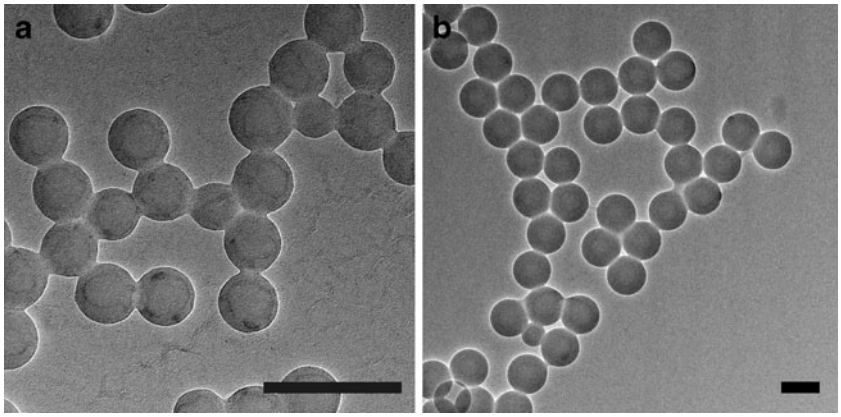

Fig. 2 Representative transmission electron micrographs of poly(D,L-lactide-*co*-glycolide) nanoparticles with mean hydrodynamic diameters of 100 (**a**) and 200 nm (**b**). Scale bars: 200 nm.

amounted to 97.1±3.8% (mean ± S.D., n=8) and 96.3± 2.0% (mean ± S.D., n=8), respectively (Table II).

Owing to NP aggregation during nebulization with the PARI LC SPRINT® STAR (Fig. 3), the quantification of NP concentration by transmission experiments was only carried out for the Aeroneb® Pro and eFlow®rapid nebulizer, yet revealed no relevant changes in NP concentration during nebulization (Fig. 4a and b). Similar to the described spectrophotometric assay, the NP concentration remained unchanged at ~100%, as assayed by gravimetric and fluorescence spectroscopic analysis (Fig. 4c-f). For nebulization with the air-jet device, a gradual increase in NP concentration over nebulization time was observed (Fig. 4c and e). Nebulization of PLGA100 and PLGA200 nanosuspensions of higher initial NP concentration caused a more pronounced NP concentration effect (Fig. 4d and f). Application of PLGA200 nanosuspensions led to an elevated NP concentration after 10 min of nebulization compared to PLGA100 nanosuspension of the same initial NP concentration (Fig. 4d and f). Moreover, the change in NP concentration for PLGA100 (5 mg/ml) and PLGA200 (2 and 5 mg/ml) nanosuspensions was significantly increased in comparison to the solute concentration of aerosolized isotonic NaCl solution, when using the PARI LC SPRINT® STAR nebulizer (Figs. 1a, 4d and f).

DISCUSSION

Inhalation of therapeutic aerosols is a typical example of targeted drug therapy offering several advantages over other routes of administration (e.g. high local concentration, reduced side effects) (30). In the past, aerosol generation from aqueous formulations was mainly subject to pneumatic- and ultrasound-driven nebulizers (13). Recent nebulizer designs employ actuated perforated plates for aerosol generation (14,15). Depending on the differing mode of operation variable aerodynamic and output characteristics are

Table III Aerodynamic and Output Characteristics of poly(D,L-lactide-*co*-glycolide) (PLGA) Nanoparticles (NP) Aerosolized with Different Nebulizer Units. The Asterisks Denote Statistically Significant Differences ($p<0.05$) Compared to Nebulized Isotonic NaCl Solution (Table I). Values are Presented as Mean ± S.D. ($n\geq4$)

Nebulizer unit	NP formulation	NP concentration/mg/ml	VMD[a]/μm	GSD[b]	FPF[c]/%	Output rate/g/min
PARI LC SPRINT® STAR	PLGA100	1	3.2±0.1	1.67±0.02*	86.1±1.7	0.07±0.01
	PLGA100	2	3.0±0.2	1.64±0.03*	88.6±3.6	0.07±0.02
	PLGA100	5	3.2±0.2	1.70±0.10	86.6±4.5	0.08±0.04
	PLGA200	1	3.1±0.1	1.71±0.04*	88.0±2.1	0.08±0.02
	PLGA200	2	3.4±0.4	1.67±0.05*	83.2±7.4	0.08±0.03
	PLGA200	5	3.2±0.3	1.68±0.06*	85.4±4.0	0.08±0.03
Aeroneb® Pro	PLGA100	1	5.8±0.2	1.90±0.04	44.4±2.6	0.35±0.03*
	PLGA100	2	5.8±0.3	1.85±0.08	43.8±3.2	0.29±0.06*
	PLGA100	5	5.9±0.1*	1.82±0.04	42.4±1.7*	0.25±0.04*
	PLGA200	1	5.6±0.3	1.82±0.05	46.0±3.4	0.24±0.06*
	PLGA200	2	5.5±0.1	1.70±0.01*	46.2±2.7	0.22±0.04*
	PLGA200	5	5.5±0.2	1.72±0.02*	45.9±2.3	0.21±0.08*
eFlow®rapid	PLGA 100	2	4.6±0.2	1.60±0.01	61.2±3.1	0.52±0.10*

[a] Volume median diameter; [b] geometric standard deviation; [c] fine particle fraction

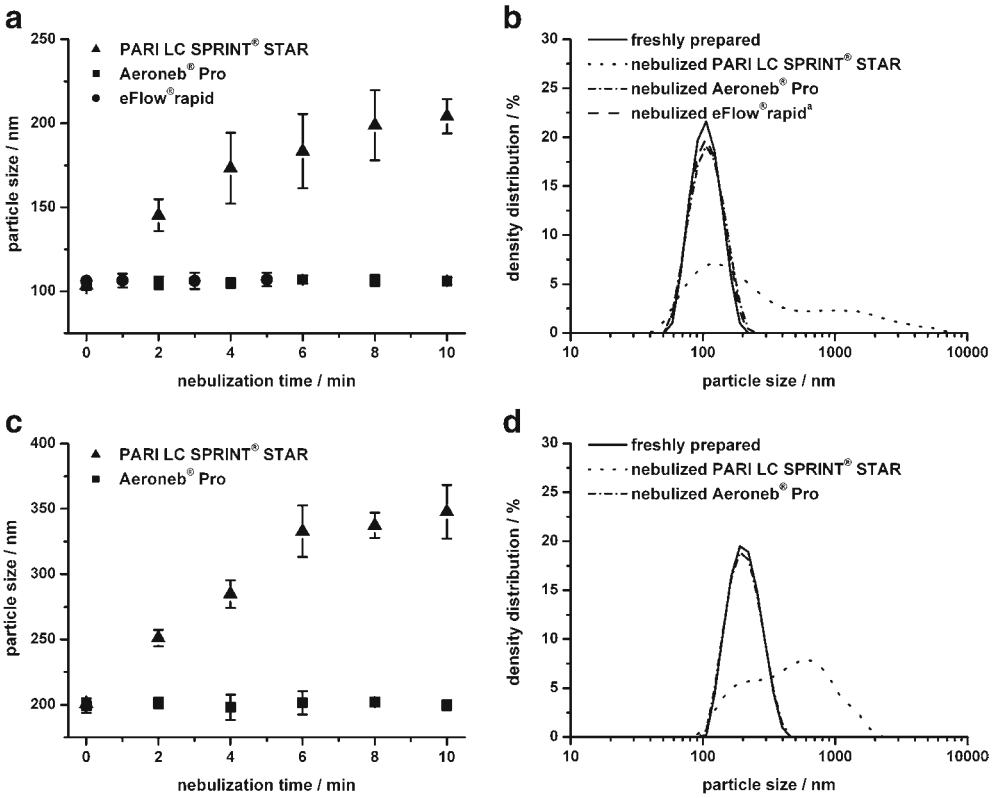

Fig. 3 Stability of poly(D,L-lactide-*co*-glycolide) (PLGA) nanoparticles (NP) (2 mg/ml) to air-jet (PARI LC SPRINT® STAR) and vibrating-membrane (Aeroneb® Pro and eFlow®rapid) nebulization (**a**, **c**), as followed by dynamic light scattering (DLS). Values are presented as mean ± S.D. (n=4). Representative particle size distribution curves from DLS for freshly-prepared NP and NP nebulized for 10 min are shown in (**b**) and (**d**). [a] Density distribution after 5 min of nebulization (**b**).

obtained for the same formulation (Table I) (13). Nevertheless, all employed nebulizers produced aerosols suitable for deep lung deposition (31). The increase in solute concentration during air-jet nebulization observed in the current study was attributed to evaporative loss of solvent during the nebulization process (12,13), which increases dramatically as additional gas is passed through the device (Fig. 1a). In contrast, both vibrating-membrane nebulizers revealed no solute concentration (Fig. 1b). Owing to the specific mechanism of aerosol generation (utilization of an actuated perforated plate) (14,15) and a marginal temperature increase of the reservoir fluid (32), solvent evaporation is minimized, thus ensuring a remarkably unchanged solute concentration throughout the time course of nebulization.

The development of controlled drug delivery vehicles is of high relevance in the field of pulmonary research (10). In this context, nanotechnology offers novel concepts for the development of optimized therapeutic and diagnostic tools for the treatment of severe diseases (33,34). Colloids have been widely investigated as potential formulations, due to their numerous advantages (e.g. targeted and controlled drug release potential) (35). Besides other approaches, biodegradable NP have shown promise for pulmonary applications (6,7,9,10,17). Nanoprecipitation is a convenient method for the preparation of specified NP from preformed polymers (26,36). Adjustment of the experimental conditions (i.e. choice of organic solvent and polymer concentration in the organic phase) enabled the fabrication of 100 and 200 nm NP composed of PLGA with narrow size distributions (Table II, Fig. 2). Moreover, encapsulation of coumarin 6 was possible at high encapsulation efficiencies (Table I).

Besides dry powder aerosolization of composite particles, nebulization of aqueous nanosuspensions has proven suitable for pulmonary application of NP formulations (6,10,16,17). Although aerodynamic and output characteristics of nebulized PLGA NP partially revealed significant differences compared to isotonic NaCl solution (Tables I and III), these distinct performances are expected to be of minor importance regarding pulmonary therapy (30,31).

The preservation of the properties of a drug delivery system during nebulization is a major demand to ensure its functionality. However, NP aggregation was observed during air-jet nebulization (Fig. 3). The well-known physical instability of biodegradable NP during air-jet nebulization was attributed to the applied aerosolization technique (high shear stress, refluxing of nanosuspension) (20,21,24). Concentration alterations, characteristic for air-jet nebulization were monitored over the time course of nebulization. As described for solutions (12), NP concentration increased during nebulization employing the PARI LC SPRINT® STAR (Fig. 4). Consistent retention effects were observed for dispersed microparticles during air-jet nebulization, which were explained on the one hand by an evaporative loss of solvent and on the other hand by the geometric size of the microparticles (25). Hence, one would expect a higher

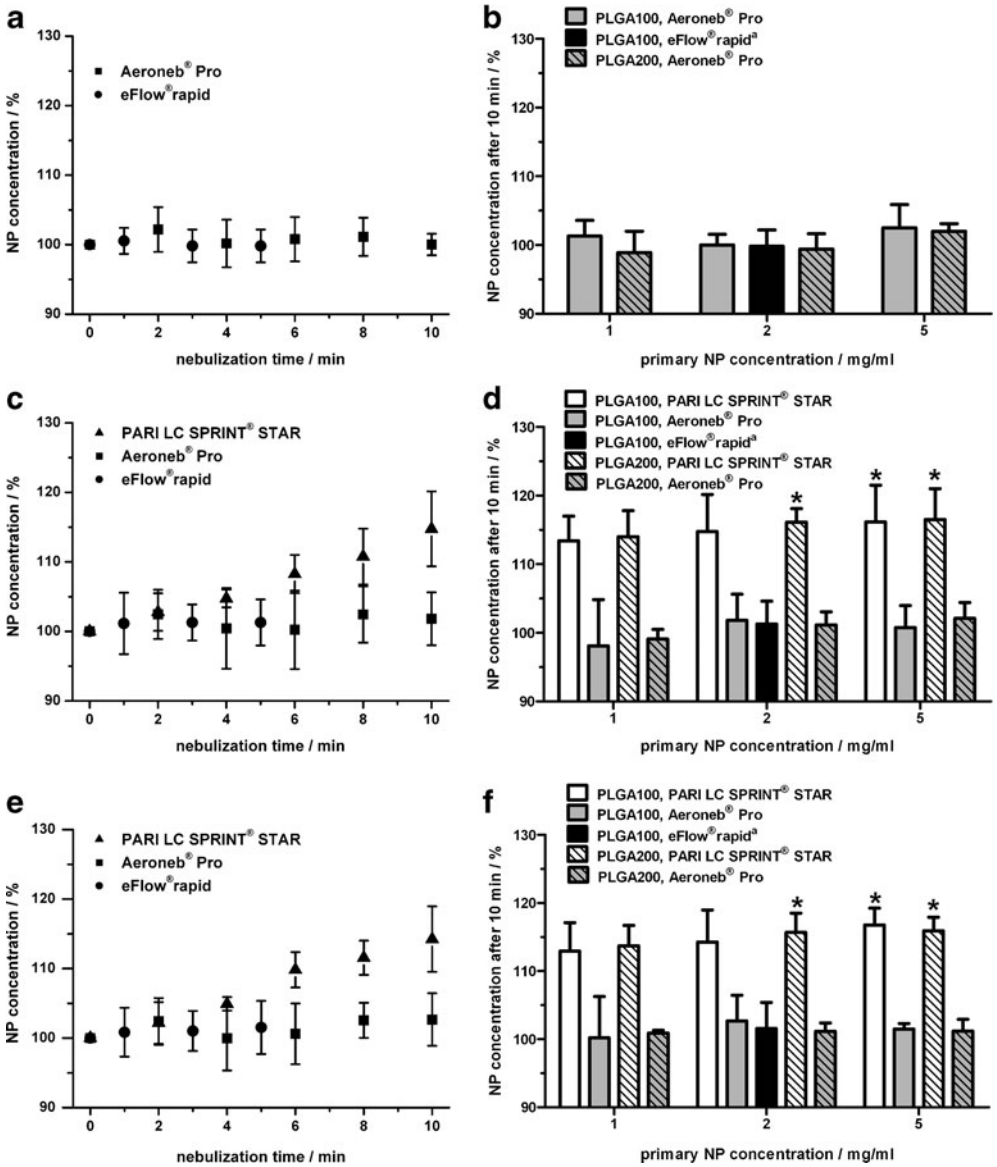

Fig. 4 Influence of nebulization time on the concentration of poly (D,L-lactide-*co*-glycolide) (PLGA) nanoparticles (NP) with nominal sizes of 100 and 200 nm in the reservoirs of the air-jet (PARI LC SPRINT® STAR) and vibrating-membrane (Aeroneb® Pro and eFlow®rapid) devices, as assessed by spectrophotometry (**a**, **b**), gravimetric analysis (**c**, **d**) and fluorescence spectroscopy (**e**, **f**). The time courses of nebulization shown in (**a**), (**c**) and (**e**) were performed with PLGA100 NP at a concentration of 2 mg/ml. The asterisks denote statistically significant differences ($p < 0.05$) compared to nebulized isotonic NaCl solution concentration effects (Fig. 1**a**). Values are presented as mean ± S.D. (n=4). [a] NP concentration after 5 min of nebulization (**b**, **d**, **f**).

output of smaller particles during air-jet nebulization. Nevertheless, the concentration effect for nanosuspensions was elevated compared to isotonic NaCl solution (Figs. 1a and 4). Moreover, the change of NP concentration was more pronounced, when a higher initial NP concentration (PLGA100, 5 mg/ml) or larger NP (PLGA200, 2 and 5 mg/ml) were utilized, hinting at another mechanism beside solvent evaporation responsible for the amplified NP concentration. The difference in NP concentration during nebulization is most likely attributed to NP aggregation in the PARI LC SPRINT® STAR device (Fig. 3). As the size of NP aggregates approaches or exceeds the aerosol droplet diameter, the amount of delivered NP vanishes.

As an alternative to air-jet nebulization, aqueous formulations can be delivered to the lung by means of vibrating-membrane technology (13–15). The application of actuated perforated plates has been recommended for aerosolization of NP formulations, as these devices avoid high shear stress during aerosolization and consequently reduce the particle aggregation tendency (10,23). None of the employed NP formulations was adversely affected utilizing the Aeroneb® Pro and eFlow®rapid nebulizer (Fig. 3). Moreover, the concentration of NP formulations remained unchanged during vibrating-membrane nebulization (Fig. 4). For aerosol generation, vibrating-membrane nebulizers use actuated perforated plates, which contain tapered holes with large cross-sections on the reservoir side (~30 µm) and a narrow cross-section on the side (~2–5 µm) from where the aerosol droplets emerge (14,15). As the generated particles revealed sizes in the submicron range (100 and 200 nm), they were capable to physically pass through the apertures of the vibrating membrane. Other formulations may be susceptible to the sieving effect of nebulization when the formulation cannot pass the aperture (initial geometric particle

diameter ≥ tapered hole diameter; aggregation during nebulization), emphasizing that suspensions should only be nebulized with a suitable vibrating-membrane device.

CONCLUSION

Drug delivery vehicles composed of submicron biodegradable particles have been frequently utilized to improve pulmonary drug delivery. Nebulization of these formulations from aqueous suspensions is an appropriate method for the formation of NP-containing aerosols. Although the aerodynamic performance of aerosolized formulations represents a solid basis for the selection of appropriate nebulizer systems, as these parameters determine pulmonary deposition patterns, the effectiveness of nebulization therapy by means of colloidal drug delivery vehicles depends on both their stability to nebulization and output in aerosol form from the nebulizer reservoir. In this regard, the current study aimed to identify a suitable nebulizer platform for the aerosol delivery of biodegradable NP avoiding particle aggregation and concentration during nebulization. Air-jet nebulization failed to effectively aerosolize biodegradable NP, as aggregation occurred during nebulization and moreover, the majority of the suspended particles were retained in the nebulizer reservoir. The beneficial mode of vibrating-membrane technology was found to be suitable for nebulization of biodegradable NP, with no apparent signs of aggregation or concentration. Overall, the results from the current study underline the suitability of vibrating-membrane nebulizers for the delivery of aerosolized biodegradable NP to the respiratory tract.

ACKNOWLEDGMENTS AND DISCLOSURES

The authors would like to thank Michael Hellwig and Andreas K. Schaper (Department of Geosciences and Materials Science Center, University of Marburg) for their support with TEM. This study was supported by the German Research Foundation (DFG). We want to express our sincere thanks for this grant.

The authors disclose that no conflicting interests associated with the manuscript exist.

REFERENCES

1. Olschewski H, Simonneau G, Galie N, Higenbottam T, Naeije R, Rubin LJ, *et al.* Inhaled iloprost for severe pulmonary hypertension. N Engl J Med. 2002;347:322–9.
2. Patton JS, Byron PR. Inhaling medicines: Delivering drugs to the body through the lungs. Nat Rev Drug Discov. 2007;6:67–74.
3. van der Schans CP. Bronchial mucus transport. Respir Care. 2007;52:1150–8.
4. Geiser M. Update on macrophage clearance of inhaled micro- and nanoparticles. J Aerosol Med. 2010;23:207–17.
5. Gessler T, Seeger W, Schmehl T. The potential for inhaled treprostinil in the treatment of pulmonary arterial hypertension. Ther Adv Respir Dis. 2011;5:195–206.
6. Beck-Broichsitter M, Gauss J, Packhaeuser CB, Lahnstein K, Schmehl T, Seeger W, *et al.* Pulmonary drug delivery with aerosolizable nanoparticles in an ex vivo lung model. Int J Pharm. 2009;367:169–78.
7. Beck-Broichsitter M, Gauss J, Gessler T, Seeger W, Kissel T, Schmehl T. Pulmonary targeting with biodegradable salbutamol-loaded nanoparticles. J Aerosol Med. 2010;23:47–57.
8. Nielsen EJB, Nielsen JM, Becker D, Karlas A, Prakash H, Glud SZ, *et al.* Pulmonary gene silencing in transgenic EGFP mice using aerosolised chitosan/siRNA nanoparticles. Pharm Res. 2010;27:2520–7.
9. Rytting E, Bur M, Cartier R, Bouyssou T, Wang X, Krueger M, *et al. In vitro* and *in vivo* performance of biocompatible negatively-charged salbutamol-loaded nanoparticles. J Controlled Release. 2010;141:101–7.
10. Beck-Broichsitter M, Merkel OM, Kissel T. Controlled pulmonary drug and gene delivery using polymeric nano-carriers. J Controlled Release. 2011:doi:10.1016/j.jconrel.2011.1012.1004.
11. Dolovich MB, Dhand R. Aerosol drug delivery: developments in device design and clinical use. Lancet. 2011;377:1032–45.
12. Steckel H, Eskandar F. Factors affecting aerosol performance during nebulization with jet and ultrasonic nebulizers. Eur J Pharm Sci. 2003;19:443–55.
13. Watts AB, McConville JT, Williams III RO. Current therapies and technological advances in aqueous aerosol drug delivery. Drug Dev Ind Pharm. 2008;34:913–22.
14. Lass JS, Sant A, Knoch M. New advances in aerosolised drug delivery: vibrating membrane nebuliser technology. Expert Opin Drug Delivery. 2006;3:693–702.
15. Waldrep JC, Dhand R. Advanced nebulizer designs employing vibrating mesh/aperture plate technologies for aerosol generation. Curr Drug Delivery. 2008;5:114–9.
16. Chow AHL, Tong HHY, Chattopadhyay P, Shekunov BY. Particle engineering for pulmonary drug delivery. Pharm Res. 2007;24:411–37.
17. Sung JC, Padilla DJ, Garcia-Contreras L, VerBerkmoes JL, Durbin D, Peloquin CA, *et al.* Formulation and pharmacokinetics of self-assembled rifampicin nanoparticle systems for pulmonary delivery. Pharm Res. 2009;26:1847–55.
18. Lebhardt T, Roesler S, Uusitalo HP, Kissel T. Surfactant-free redispersible nanoparticles in fast-dissolving composite microcarriers for dry-powder inhalation. Eur J Pharm Biopharm. 2011;78:90–6.
19. Beck-Broichsitter M, Schweiger C, Schmehl T, Gessler T, Seeger W, Kissel T. Characterization of novel spray-dried polymeric particles for controlled pulmonary drug delivery. J Controlled Release. 2012;158:329–35.
20. Dailey LA, Kleemann E, Wittmar M, Gessler T, Schmehl T, Roberts C, *et al.* Surfactant-free, biodegradable nanoparticles for aerosol therapy based on the branched polyesters, DEAPA-PVAL-g-PLGA. Pharm Res. 2003;20:2011–20.
21. Dailey LA, Schmehl T, Gessler T, Wittmar M, Grimminger F, Seeger W, *et al.* Nebulization of biodegradable nanoparticles: Impact of nebulizer technology and nanoparticle characteristics on aerosol features. J Controlled Release. 2003;86:131–44.
22. Packhäuser CB, Lahnstein K, Sitterberg J, Schmehl T, Gessler T, Bakowsky U, *et al.* Stabilization of aerosolizable nano-carriers by freeze-drying. Pharm Res. 2009;26:129–38.
23. Beck-Broichsitter M, Kleimann P, Gessler T, Seeger W, Kissel T, Schmehl T. Nebulization performance of biodegradable sildenafil-loaded nanoparticles using the Aeroneb® Pro: Formulation

aspects and nanoparticle stability to nebulization. Int J Pharm. 2012;422:398–408.
24. Hureaux J, Lagarce F, Gagnadoux F, Vecellio L, Clavreul A, Roger E, *et al*. Lipid nanocapsules: Ready-to-use nanovectors for the aerosol delivery of paclitaxel. Eur J Pharm Biopharm. 2009;73:239–46.
25. McCallion ONM, Taylor KMG, Thomas M, Taylor AJ. Nebulisation of monodisperse latex sphere suspensions in air-jet and ultrasonic nebulisers. Int J Pharm. 1996;133:203–14.
26. Beck-Broichsitter M, Rytting E, Lebhardt T, Wang X, Kissel T. Preparation of nanoparticles by solvent displacement for drug delivery: A shift in the "ouzo region" upon drug loading. Eur J Pharm Sci. 2010;41:244–53.
27. Mitchell JP, Nagel MW, Nichols S, Nerbrink O. Laser diffractometry as a technique for the rapid assessment of aerosol particle size from inhalers. J Aerosol Med. 2006;19:409–33.
28. Hinds WC. Aerosol technology: properties, behavior, and measurements of airborne particles. New York: Wiley; 1998.
29. Beck-Broichsitter M, Thieme M, Nguyen J, Schmehl T, Gessler T, Seeger W, *et al*. Novel'nano in nano' composites for sustained drug delivery: Biodegradable nanoparticles encapsulated into nanofiber non-wovens. Macromol Biosci. 2010;10:1527–35.
30. Groneberg DA, Witt C, Wagner U, Chung KF, Fischer A. Fundamentals of pulmonary drug delivery. Respir Med. 2003;97:382–7.
31. Carvalho TC, Peters JI, Williams III RO. Influence of particle size on regional lung deposition: what evidence is there? Int J Pharm. 2011;406:1–10.
32. Fink JB, Power J. Comparison of a novel aerosol generator with a standard ultrasonic nebulizer designed for use during mechanical ventilation (Abstract). Am J Respir Crit Care Med. 2001;163:A127.
33. LaVan DA, Lynn DM, Langer R. Moving smaller in drug discovery and delivery. Nat Rev Drug Discov. 2002;1:77–84.
34. Farokhzad OC, Langer R. Impact of nanotechnology on drug delivery. ACS Nano. 2009;3:16–20.
35. Couvreur P, Vauthier C. Nanotechnology: Intelligent design to treat complex disease. Pharm Res. 2006;23:1417–50.
36. Vauthier C, Bouchemal K. Methods for the preparation and manufacture of polymeric nanoparticles. Pharm Res. 2009;26:1025–58.